

Fig. 5. The left tibia. A typical example of a long bone from the male skeleton: nearly intact, with minimal warping and a step transverse fracture, which are all evidence of a dry bone



cremation consistent with the taphonomic history of Arrhidaeus. Note that the step fracture in the distal part of the tibia extends from the end of the longitudinal crack across the shaft of the bone.

bones is excellent, with minimal warping and transverse cracking that is straight (Fig. 5). The skeleton is almost complete (11), and light brown is the dominant color of the bones. Only the left proximal ulna presents some curved transverse fractures, probably the result of insufficient decomposition in this area. The right ulna is nearly perfect, with a longitudinal crack. This type of preservation of the male skeleton shows that most of the bones were dry when cremated; that is, they were buried for some time before they were cremated. This is consistent with the taphonomic history of inhumation, cremation, and reinterment that only the bones of Arrhidaeus underwent, as already mentioned. Nevertheless, Musgrave reported that the bones appear sufficiently warped to have been burned fleshed (11), although he accepts the near-completeness and the huge size of many bones (6), the lack of transverse breaks, and the slight warping of many bones (6), despite his own experiments in a kiln with a dry radius that showed no transverse cracking (13). To explain the good preservation of these bones, he suggested a different cremation technique (13): burning in a brick box constructed around the body (6). But of course the real reason for the good preservation is the conspicuous lack of transverse cracks in many of the bones.

King Philip II suffered severe injuries, but there is no skeletal evidence whatsoever of any injuries to the male occupant of Royal Tomb II at Vergina, especially in the orbital bones. The reported facial injuries and asymmetries are mainly the result of cremation and poor reconstruction of the skull; there is thus strong anthropological evidence against a Philip II identification. The skeletal evidence that shows a dry bone cremation leaves no room for doubt that Royal Tomb II belongs to Philip III Arrhidaeus. This is consistent with the archaeological evidence that points to a later date (2, 3) for Royal Tomb II. In this case, some of the artefacts of Royal Tomb II may belong to Alexander the Great (2), which Philip III Arrhidaeus inherited from his half-brother Alexander in Babylon and brought back to Macedonia (2), where he was buried with them as the last king of the Argeads.

References and Notes

1. M. Andronicos, *Vergina: The Royal Tombs* (Ekdotike Athinon, Athens, Greece, 1994).
2. E. N. Borza, *Phoenix* 41, 105 (1987); *In the Shadow of Olympus. The Emergence of Macedon* (Princeton Univ. Press, Princeton, NJ, 1992).
3. The archaeological evidence itself now weighs strongly in favor of a post-Philip II identification. In their recent work on the Derveni tombs, which date to the late 4th century B.C., P. Themelis and J. Touratsoglou [*The Derveni Tombs* (Publication 59, TAPA, Athens, Greece, 1997)] describe pottery similar to that in Tomb II at Vergina, thus moving the date of Vergina Royal Tomb II down to the generation after the death of Philip II. See also O. Palagia, *Minerva* 9, 25 (1998). Palagia's views are expanded in her article "Hephaestion's Pyre and the Royal Hunt of Alexander," in *Alexander the Great: Fact and Fiction*, A. B. Bosworth and E. J. Baynham, Eds. (Oxford Univ. Press, Oxford, 2000).
4. N. I. Xirotiris and F. Langenscheidt, *Archaiologike Ephemeris* 1981, 142 (1981).
5. A. S. Riginos, *J. Hell. Stud.* 114, 103 (1994). It is not clear whether Philip II's left or right arm was maimed.
6. A. J. N. W. Prag, J. H. Musgrave, R. A. H. Neave, *J. Hell. Stud.* 104, 60 (1984).
7. J. Prag and R. Neave, *Making Faces, Using Forensic and Archaeological Evidence* (British Museum Press, London, 1997), pp. 53–84.
8. A. J. N. W. Prag, *Am. J. Archaeol.* 94, 237 (1990).

9. B. K. B. Berkovitz and B. J. Moxham, *Color Atlas of the Skull* (Mosby-Wolfe, London, 1989).
10. See, for example, T. D. White and P. A. Folkens, *Human Osteology* (Academic Press, San Diego, CA, 1991), fig. 4.2; G. Hauser and G. F. De Stefano, *Epigenetic Variants of the Human Skull* (E. Schweizerbart'sche Verlagsbuchhandlung, Stuttgart, Germany, 1989), plate VIII.
11. J. H. Musgrave, in *Current Topics in Oral Biology*, S. J. Lisney and B. Matthews, Eds. (Univ. of Bristol Press, Bristol, UK, 1985), pp. 1–16.
12. N. Xirotiris, who did the reconstruction of the face, said on Greek television in 1999 that he was the one who misreconstructed the maxilla, that it was the best one could do at the time to preserve and support these delicate parts of the facial anatomy, and that it was probably this reconstruction that misled Musgrave. Indeed, the facial surgeons J. Lendum and E. Curphey, who first suggested the antemortem asymmetry of the face (7), examined only the casts of the mandible and the maxilla. The consolidants and glues Xirotiris used are reversible.
13. J. Musgrave, *Annu. Br. Sch. Athens* 85, 271 (1990).
14. W. L. Adams, *Ancient World* 22, 27 (1991).
15. T. D. Stewart, *Essentials of Forensic Anthropology* (Thomas, Springfield, IL, 1979), pp. 59–68; D. H. Ubelaker, *Human Skeletal Remains* (Taraxacum, Washington, DC, 1991); N. P. Herrmann and J. L. Bennett, *J. Forensic Sci.* 44, 461 (1999).
16. See, for example, P. Shipman, *Life History of a Fossil. An Introduction to Taphonomy and Paleoecology* (Harvard Univ. Press, Cambridge, MA, 1981).
17. D. W. Von Endt and D. J. Ortner, *J. Archaeol. Sci.* 11, 247 (1984).
18. P. E. Hare, in *Fossils in the Making. Vertebrate Taphonomy and Paleoecology*, A. K. Behrensmeier and A. P. Hill, Eds. (Univ. of Chicago Press, Chicago, IL, 1980), pp. 208–219.
19. I thank A. Kottaridou for allowing me to study the male skeleton of Royal Tomb II and M. Teliopoulou for curating it during the study.

11 November 1999; accepted 14 January 2000

Emergence of Genetic Instability in Children Treated for Leukemia

B. A. Finette,^{1,2,3*} A. C. Homans,^{1,3} R. J. Albertini^{2,3,4}

T cells from patients who had received chemotherapy for B-lineage acute lymphocytic leukemia were studied to determine whether genetic instability, a principal characteristic of cancer cells, can also occur in nonmalignant cells. Consistent with expectations for a genetic instability phenotype, multiple mutations were detected in the hypoxanthine-guanine phosphoribosyltransferase (*HPRT*) reporter gene in independently isolated mutant T cells expressing identical rearranged T cell receptor β (*TCR β*) gene hypervariable regions. These results indicate that cancer treatment can lead to genetic instability in nonmalignant cells in some individuals. They also suggest a mechanistic paradigm for the induction of second malignancies and drug resistance.

Carcinogenesis is a multistep process in which somatic cells acquire a series of stable genetic mutations in a specific clonal lineage. How multiple mutations accumulate in the same cell over a clinically relevant time period remains unclear, because individual spontaneous mutations ($\sim 1 \times 10^{-5}$ to 1×10^{-7} mutation per cell division) occur at low rates in vivo. One hypothesis states that genetic instability develops early to produce an increased

rate of mutations in a distinct clone (1, 2); another postulates that multiple mutations simply accumulate as a consequence of extensive clonal proliferation (3). In either case, genetic instability likely involves cellular changes that affect the expression and/or function of cell cycle (4–6), cell death (7), and DNA repair pathways (8). These cellular changes have been presumed to be unique to premalignant or frankly malignant cells. The purpose of this

REPORTS

study was to investigate whether genetic instability can also occur in nonmalignant cells from patients who have received chemotherapy for B-lineage acute lymphocytic leukemia (ALL). We addressed this by characterizing mutations in the hypoxanthine-guanine phosphoribosyltransferase (*HPRT*) gene in T cells.

We studied 103 patients with ALL: 19 at initial diagnosis before chemotherapy, 32 in complete remission, and 58 at the time of relapse before retreatment (9). Treatments included methotrexate, prednisone, and long-term use of purine analogs such as 6-thioguanine and 6-mercaptopurine, which positively select in vivo for cells deficient in *HPRT* activity. Two patients also received cyclophosphamide.

T cell mutant frequencies (Mfs) were determined by the *HPRT* cloning assay (10) (Table 1). Mfs for the 19 patients studied at diagnosis (1 to 18 years of age) ranged from 0.2 to 3.4×10^{-6} with a mean of 1.23×10^{-6} , values that are not statistically different from controls (11). Mfs for patients in remission (4 to 37 years of age) ranged from 3.3 to 4304×10^{-6} with a mean of 331×10^{-6} , whereas those for patients at relapse (2 to 21 years of age) ranged from 1 to 4941×10^{-6} , with a mean of 303×10^{-6} . These Mf values are significantly elevated compared with controls and ALL patients before treatment ($P < 0.001$) (Table 1) (12). Ten of 32 patients in remission (31%), and 14 of 58 patients at relapse (24%), had Mfs that were >30-fold higher than age-matched controls. These are presented graphically in Fig. 1 and confirm earlier observations of elevated *HPRT* Mfs in patients treated for ALL (13, 14).

Genetic instability, manifest as multiple mutations in clonal lineages, is most likely to be found in patients with grossly elevated Mfs. Therefore, using previously described methods (15–19), we characterized 182 *HPRT* mutant isolates recovered from 15 of the 24 patients with extremely elevated Mfs (7 of 10 patients in remission and 8 of 14 in relapse). Assigning *HPRT* mutations to specific T cell clones took advantage of the diversity of TCR β CDR3 gene rearrangements as unambiguous molecular signatures of in vivo T cell clonality (20–22). Mutant isolates from 4 of these 15 patients showed multiple *HPRT* mutational events in the same allele/molecule (23).

Molecular analysis of 21 independently isolated mutants from subject CS 44 (samples B1 and B2) revealed that two unique

HPRT mutations occurred in vivo before TCR gene rearrangement because they appeared in two or more distinct TCR gene-defined clones. The T29/30 deletion was found in three mutant clones designated by their CDR3 amino acid sequence as DSASG, VVSGRAPGG, and a third that was not characterized, whereas the IVS6+2insT mutation was found in two mutant clones, LSPGLA and ILGQ (Table 2) (23, 24). Clone VVSGRAPGG, marked by the T29/30 deletion, acquired an additional *HPRT* G¹⁶⁸ → T base substitution, and clone LSPGLA, marked by the IVS6+2insT mutation, acquired an additional exon 6 deletion. Two additional TCR gene-defined clones in this subject also had evidence of multiple *HPRT* mutational events arising in a single allele/molecule. One mutant isolate from clone AVAGAH acquired a presumed deletion of exon 5 and a G⁵⁰⁸ → A base substitution, and one mutant from clone

RGTSR acquired an IVS6+7A → T base substitution and a 38-base-pair (bp) insertion in exon 5 (23). Although it is not possible to specify the temporal order of the mutations in

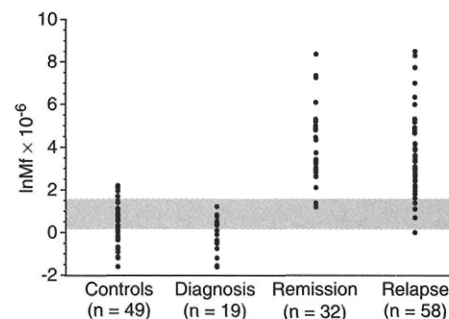


Fig. 1. Frequency of *HPRT* mutations ($\ln Mf \times 10^{-6}$) in children with ALL at diagnosis, remission, and at relapse compared with normal controls. Shaded region represents group mean for age-matched controls (0 to 21 years of age).

Table 1. T cell cloning efficiencies (CE) and *HPRT* Mfs in children with ALL.

Subjects	n	Age (years)		Months since initial diagnosis*	CE (mean)	Mf†		ln Mf (mean)	Fold increase‡
		Range	Mean			Range	Mean		
Normal	49	0.08–17	7	—	0.35	0.2–9.0	2.3	0.40	—
Diagnosis	19	1–18	5	0	0.38	0.2–3.4	1.2	-0.06	<1–3
Remission	32	4–37	15	30–322	0.24	3.3–4304	331	4.02	<1–812
Relapse	58	2–21	10	5–110	0.27	1.0–4941	303	3.49	<1–1335
Statistical comparison of ln Mf§					P value¶				
Normal vs. diagnosis					0.073				
Normal vs. remission					<0.001				
Normal vs. relapse					<0.001				
Diagnosis vs. remission					<0.001				
Diagnosis vs. relapse					<0.001				
Remission vs. relapse					0.220				

*Range of months from initial diagnosis. †Mf values $\times 10^{-6}$. ‡Calculated as $(Mf \times 10^{-6}) / (\text{mean } Mf \times 10^{-6})$ of age-matched controls: 0–5 years (1.4×10^{-6}), 6–11 years (3.5×10^{-6}), 12–16 years (3.7×10^{-6}), >18 years (5.3×10^{-6}). §For the statistical analysis, six patients in remission were excluded because they were also studied at the time of diagnosis. When these six subjects are compared with each other, the same statistically significant relationships exist. ¶P values not adjusted for multiple comparison. Values remain significant for a P value < 0.05 using a Bonferroni adjusted Mann-Whitney test for pairwise comparisons.

Table 2. Evidence for genetic instability in T cell clones from children treated for ALL.

Subject/sample	TCR β CDR3* defined clone	<i>HPRT</i> mutation		
		Mutation 1	Mutation 2	Mutation 3
CS 44 B1	VVSGRAPGG	delT ^{29/30}	G ¹⁶⁸ → T	
	LSPGLA	IVS6+2 insT	del exon 6‡	
	AVAGAH	exclusion exon 5†	G ⁵⁰⁹ → A	
	RGTSR	IVS6+7A → T	38-bp ins@382 exon 5	
CS 44 B2	LSPGLA	IVS6+2 insT†	del exon 6‡	
CS 143 B1	YVVGGA	del429–475	G ²⁹² → A	del exons 2–6‡
CS 143 B2	YVVGGA	del429–475	G ⁵² → A	
CS 63 B1	YQARTGY	C ⁵⁰⁸ → T	A ³¹ → G	
		C ⁵⁰⁸ → T	exclusion 2–6	
CS 183 B1	STNSQ	G ¹⁹⁰ → C†	del389–400	

*T cell clones are defined by the TCR β gene rearranged junctional amino acid sequences that represent the hypervariable CDR3 region. †Sequential order of mutations cannot be determined. ‡Genomic analysis of these mutant isolates revealed no splice-site or exon mutations and as a result are designated as presumed deletions because they are from female subjects.

¹Department of Pediatrics, ²Department of Microbiology and Molecular Genetics, ³Vermont Cancer Center, and ⁴Department of Medicine, University of Vermont, Medical Alumni Building, Burlington, VT 05405, USA.

*To whom correspondence should be addressed. E-mail: finette@salus.med.uvm.edu

the last two examples, their physical distance from each other argues against single complex events. Figure 2 depicts the proposed mutational sequence associated with the T cell clonal lineages found in subject CS 44.

Multiple *HPRT* mutations were also found in TCR gene–defined clones from samples B1 and B2 from subject CS 143 (23) (Table 2). In each sample, a 46-bp *HPRT* deletion (del 429–475) was found in clone YVVGGA. In this subclone, now defined by *HPRT* del 429–475, two additional *HPRT* mutations were recovered, a G²⁹² → A transition (sample B1) and a G⁵² → A transition (sample B2). Recovery of an additional mutant isolate from the YVVGGA subclone with a presumed deletion of exons 2 to 6 that obliterated all previous *HPRT* mutations suggests a third *HPRT* mutational event in this clonal lineage. Clonally restricted multiple *HPRT* mutations are also found in relapse patients CS 63 and 183 (Table 2) (23). In the former, a C⁵⁰⁸ → T mutation was found in isolates of clone YQARTGY, each marked by a different and later *HPRT* mutational event. In patient CS 183, clone STNSQ acquired two independent *HPRT* mutations in the same allele/molecule,

a G¹⁹⁰ → C and an 11-bp deletion (Table 2) (23). The temporal sequence of these events cannot be determined.

Therefore, our data show that nonmalignant T cell clones from 4 of the 15 children with tremendous elevations of *HPRT* Mfs acquired multiple mutations in the same allele/molecule. Multiple *HPRT* mutations in TCR gene–defined clones were not observed in subjects before chemotherapy or in controls. This suggests that clonally restricted genetic instability can develop after chemotherapy. The number of cell generations required to produce multiple mutations (*n*) in a single allele/molecule is the spontaneous mutation rate raised by the power of *n*. Given a spontaneous mutation rate of 10⁻⁵ to 10⁻⁷ per cell generation, about 10¹⁰ to 10²¹ cell generations would be required to accumulate two or three mutations in the same allele/molecule as found in the TCR gene–defined clones from these patients. Such mutational events would not occur in a clinically relevant time frame even if the mutation rate were increased by an order of magnitude because of genotoxic chemotherapy (25). The accumulation of multiple *in vivo* *HPRT* mutations in a T cell clone as a consequence of extensive

clonal expansion after chemotherapy cannot explain these observations. Although this scenario would result in multiple unique single mutations in a TCR gene–defined clone, it would not produce multiple mutations in a single allele/molecule. Indeed, in one of our patients we detected 10 different single mutational events in 13 independently isolated mutants from a TCR gene–defined clone in which each mutant isolate had only a single *HPRT* mutation.

We postulate that the pattern of mutations observed in our patients reflects *in vivo* evolution of genetic instability, leading to mutant phenotypes previously suggested for malignant transformation (1, 2). Multiple mutations in the p53 gene in tumor cells have been interpreted as evidence of genetic instability (26, 27). In this case, the p53 mutations were thought to provide a selective advantage. However, because established tumors contain a multitude of genetic changes, the primacy of the observed genetic instability cannot be determined.

In our study, the T cells were from patients exposed to multiple courses of chemotherapy leading to repetitive cycles of cell death followed by restorative proliferation. Such cellular responses to cytotoxic/mutagenic exposures *in vivo* may select for genetic instability analogous to that found in prokaryotic (28, 29) and eukaryotic cells (30) *in vitro* that have been sequentially exposed to genotoxic challenges. The presence of purine analogs in ALL treatment regimens ensures that *HPRT* reporter mutants are selected, making these mutations unique probes for highly mutable cells.

Although we show that genetic instability does not inevitably lead to cancer, it may play a role in the induction of second malignancies and drug resistance. Analysis of nonmalignant cells with this tumorigenic characteristic but without the multiple changes found in cancer cells may prove useful for elucidating the cellular and genetic events associated with malignant transformation.

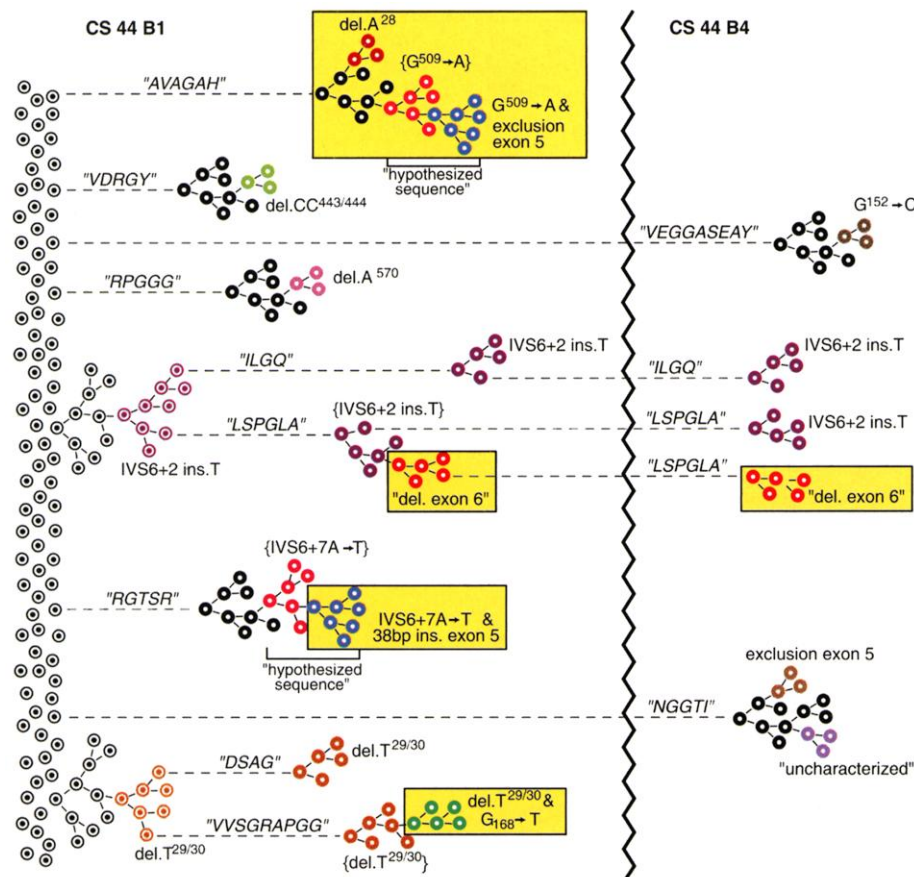


Fig. 2. Clonal lineages of *HPRT* mutant isolates from subject CS 44 demonstrating acquisition of clonally restricted multiple *HPRT* mutations. Mutant isolates were recovered at two different times within 1 year both during (CS 44 B1) and after (CS 44 B4) chemotherapy. Open circles represent undifferentiated/prethymic T cells; filled circles represent differentiated/postthymic T cells. *HPRT* mutations in brackets represent predicted but unrecovered mutant isolates. Shaded regions indicate T cell clones demonstrating multiple *HPRT* mutations in the same allele/molecule.

References and Notes

1. C. Lengauer, K. W. Kinzler, B. Vogelstein, *Nature* **396**, 643 (1998).
2. L. A. Loeb, in *Advances in Cancer Research*, G. F. Van de Woede and G. Klein, Eds. (Academic Press, San Diego, 1998) vol. 72, pp. 26–56.
3. I. Tomlinson and W. Bodmer, *Nat. Med.* **5**, 11 (1999).
4. C. H. Spruck, K.-A. Won, S. I. Reed, *Nature* **401**, 297 (1999).
5. K. W. Kinzler and B. Vogelstein, *Nature* **386**, 761 (1997).
6. T. L. Orr-Weaver and R. A. Weinberg, *Nature* **392**, 223 (1998).
7. R. G. Wickremasinghe and A. V. Hoffbrand, *Blood* **93**, 3587 (1999).
8. T. A. Kunkel, M. A. Resnick, D. A. Gordenin, *Cell* **88**, 155 (1997).
9. Peripheral blood samples were obtained from patients at the time of diagnosis with ALL and from patients previously treated for ALL at the Pediatric Oncology Clinic at the University of Vermont. Patients at the time of bone marrow relapse were also

- recruited from other Pediatric Oncology Group (POG) institutions before treatment began. Informed consent was obtained, and procedures approved by the Committee on Human Research at the University of Vermont and other POG institutions were followed.
10. Peripheral blood was separated and the mononuclear cell fraction was obtained for the T cell cloning assay within 12 to 24 hours of its collection. The T cell cloning assay and analysis have been described [see B. A. Finette *et al.*, *Mutat. Res.* **308**, 223 (1994)].
 11. B. A. Finette *et al.*, *Mutat. Res.* **308**, 223 (1994).
 12. Mutant frequencies in subjects at diagnoses, remission, and relapse were compared with normal controls by the nonparametric Kruskal-Wallis test. Pairwise differences between groups were assessed by Mann-Whitney tests, with a Bonferroni adjustment for multiple comparisons. Linear regression analysis was used to examine the relationship between the logarithm of Mf (lnMf) and months since diagnosis.
 13. H. Hirota *et al.*, *Mutat. Res.* **315**, 95 (1994).
 14. S. Koishi *et al.*, *Mutat. Res.* **422**, 213 (1998).
 15. R. A. Gibbs, P.-N. Nguyen, A. Edwards, A. B. Civitello, C. T. Caskey, *Genomics* **7**, 235 (1990).
 16. J. C. Fuscoe *et al.*, *Cancer Res.* **51**, 6001 (1991).
 17. B. A. Finette, J. P. O'Neill, P. M. Vacek, R. J. Albertini, *Nat. Med.* **4**, 1144 (1998).
 18. N. F. Cariello *et al.*, *Nucleic Acids Res.* **26**, 198 (1998).
 19. Because the *HPRT* gene is located on the X chromosome, molecular analysis at the DNA/RNA level was performed in a different way for mutant isolates from males and females [B. A. Finette, J. P. O'Neill, P. M. Vacek, R. J. Albertini, *Nat. Med.* **4**, 1144 (1998)].
 20. S. Tonegawa, *Nature* **302**, 575 (1983).
 21. R. J. Albertini, J. A. Nicklas, T. R. Skopec, L. Recio, J. P. O'Neill, *Mutat. Res.* **400**, 381 (1998).
 22. To determine the clonality of peripheral *HPRT* mutant T cell clones we performed a two-step polymerase chain reaction (PCR) with about 10⁴ cells from each isolate to perform a reverse transcriptase-PCR amplification followed by a TCR β gene hot start PCR with a V β and C β consensus primer mix. The resulting PCR product was purified and the highly polymorphic CDR3/variable regions of TCR β were sequenced.
 23. Supplementary material is available at www.sciencemag.org/feature/data/1047822.shl
 24. Single-letter abbreviations for amino acid residues are as follows: A, Ala; C, Cys; D, Asp; E, Glu; F, Phe; G,

- Gly; H, His; I, Ile; K, Lys; L, Leu; M, Met; N, Asn; P, Pro; Q, Gln; R, Arg; S, Ser; T, Thr; V, Val; W, Trp; and Y, Tyr.
25. R. F. Branda, J. P. O'Neill, L. M. Sullivan, R. J. Albertini, *Cancer Res.* **51**, 6603 (1991).
 26. B. S. Strauss, *Carcinogenesis* **18**, 1445 (1997).
 27. B. S. Strauss, *Semin. Cancer Biol.* **6**, 431 (1998).
 28. J. H. Miller, *Annu. Rev. Microbiol.* **50**, 625 (1996).
 29. E. F. Mao, L. Lane, J. Lee, J. H. Miller, *J. Bacteriol.* **179**, 417 (1997).
 30. C. R. Hunt *et al.*, *Cancer Res.* **58**, 3986 (1998).
 31. Supported by National Institute of Child Health & Human Development grant 1R29HD35309, National Cancer Institute (NCI) grant 1K01CA77737, grant 6103-98 from the Leukemia Society of America, the Lake Champlain Cancer Research Organization, the Vermont Chapter of the American Cancer Society, the Art Ehrmann Cancer Fund and NCI grant P30CA22435 to the University of Vermont Cancer Center DNA Analysis Facility. We thank C.-C. Durieux-Lu, H. Kendall, and J. Rivers for technical assistance; S. Billado for assistance with blood samples; and P. Vacek for statistical analyses.

9 December 1999; accepted 28 February 2000

Homologs of Small Nucleolar RNAs in Archaea

Arina D. Omer,¹ Todd M. Lowe,^{2*} Anthony G. Russell,¹ Holger Ehardt,¹ Sean R. Eddy,² Patrick P. Dennis^{1†}

In eukaryotes, dozens of posttranscriptional modifications are directed to specific nucleotides in ribosomal RNAs (rRNAs) by small nucleolar RNAs (snoRNAs). We identified homologs of snoRNA genes in both branches of the Archaea. Eighteen small sno-like RNAs (sRNAs) were cloned from the archaeon *Sulfolobus acidocaldarius* by coimmunoprecipitation with archaeal fibrillarin and NOP56, the homologs of eukaryotic snoRNA-associated proteins. We trained a probabilistic model on these sRNAs to search for more sRNAs in archaeal genomic sequences. Over 200 additional sRNAs were identified in seven archaeal genomes representing both the Crenarchaeota and the Euryarchaeota. snoRNA-based rRNA processing was therefore probably present in the last common ancestor of Archaea and Eukarya, predating the evolution of a morphologically distinct nucleolus.

Ribosome biogenesis in Eukarya occurs in the nucleolus. Several nucleolar proteins (NOPs), including fibrillarin, Nop56, and Nop58, and dozens of snoRNAs are involved in this process (1). The snoRNAs fall into two major classes: C/D box and H/ACA box RNAs. The C/D box snoRNAs are efficiently precipitated with antibodies against fibrillarin. Most C/D box snoRNAs target specific ribose methylations within rRNA, whereas most H/ACA box RNAs target specific conversions of uridine to pseudouridine within rRNA (2).

The general mechanism of C/D box

snoRNA-targeted ribose methylation has been well established. Each snoRNA contains a 9- to 21-nucleotide (nt)-long sequence, located 5' to the D or D' box motif, that is complementary to an rRNA target sequence. Methylation is directed to the rRNA nucleotide that participates in the base pair 5 nt upstream from the start of the D or D' box. It is likely that most, if not all, eukaryotic rRNA ribose methylations are guided by snoRNAs. In the yeast *Saccharomyces cerevisiae*, methylation guide snoRNAs have been assigned to all but four of the 55 rRNA ribose methylation sites (3).

SnoRNAs, which are apparently ubiquitous in Eukarya, have not been found in Bacteria or Archaea. However, the rRNA of the archaeon *Sulfolobus solfataricus* (*Sso*) has been shown to contain 67 ribose methylation sites, a number similar to that found in eukaryotes (4). Even though Archaea are unicellular prokaryotic organisms that lack a nucleolus, their genomes encode homologs to the essential eukaryotic nucleolar proteins,

fibrillarin and NOP56/58 (5, 6). On the basis of these observations, we decided to examine Archaea for the presence of sno-like RNAs (sRNAs).

To isolate sRNAs from the archaeon *Sulfolobus acidocaldarius* (*Sac*), we cloned the *S. acidocaldarius* homologs of the eukaryotic fibrillarin and NOP56/58 proteins, designated aFIB and aNOP56, using sequence information from a related species, *S. solfataricus* (7). The cloned genes were expressed in *Escherichia coli*, and the recombinant proteins were purified and used to raise polyclonal antibodies in rabbits. The two antibody preparations were each highly specific and recognize single polypeptides of the predicted size in total *S. acidocaldarius* cell extracts (Fig. 1A). The antibodies were used to monitor the size distribution of particles containing aFIB and aNOP56 in a glycerol gradient fractionation of partially purified cell lysate (Fig. 1A) (8). Both aFIB and aNOP56 sedimented as a large heterogeneous complex.

To detect RNAs that associate with aFIB- and aNOP56-containing complexes, we immunoprecipitated aliquots from gradient fractions with either antibody to aFIB or antibody to aNOP56. Total RNA was extracted with phenol from the supernatants and the pellets, and a portion from each was 3' end-labeled with ³²P-cytidine-5',3'-bis-phosphate (pCp) and displayed by denaturing polyacrylamide gel electrophoresis (Fig. 1, B and C). The most abundant RNAs that were coimmunoprecipitated appear as a family of bands ranging in length from about 50 to 70 nt. This size class of RNAs, which is substantially shorter than eukaryotic C/D box snoRNAs, was invisible when total cellular RNA was labeled with pCp. To obtain cDNA clones, we gel-purified the RNAs precipitated from fraction 5 with antibody to aFIB and from

¹Department of Biochemistry and Molecular Biology, University of British Columbia, 2146 Health Sciences Mall, Vancouver, BC V6T 1Z3, Canada. ²Department of Genetics, Washington University School of Medicine, 4566 Scott Avenue, St. Louis, MO 63110, USA.

*Present address: Department of Genetics, M322, Stanford University School of Medicine, 300 Pasteur Drive, Stanford, CA 94305-5120, USA.

†To whom correspondence should be addressed. E-mail: patrick.p.dennis@ubc.ca